CHAPTER 76

FIELD STUDY OF A TIDAL INLET, BIMINI, BAHAMAS[1]

W HARRISON, R J BYRNE, J D BOON, III, and R W MONCURE
Division of Physical, Chemical, and Geological Oceanography
Virginia Institute of Marine Science, Gloucester Point, Virginia 23062

ABSTRACT

The inlet bathymetry was mapped by standard photogrammetric techniques after photographing the bottom directly through the water column The channel bottom is bare beachrock or is floored with bioclastic sands and gravels (S G = 2 84)

A nine-day time series of observations of current speed and direction, and water temperature and salinity was obtained at two depths at each of eight stations using tripod-mounted, telemetering sensor packages Twelve-to-18-minute pulsations in the flow were often observed Spectral analysis of near-surface current speeds shows significant peaks at 2 4, 3 2, 4 3, 6 7, and 12 3 hrs

Evolution of sand ripples and dunes was monitored over a 200-ft distance during one tidal cycle The pattern of growth illustrates the differences in bedform geometry which may be expected to influence friction coefficients Evidence is presented for a bottom jet that is induced by flow over the crests of sand waves

Tracer sand, sorted into two size groups and color-coded for identification, was released on a flood current Sampling of color-coded tracer sand was conducted by divers using strips of grease-coated plastic tape Spatial distribution of tracers in relation to the bedforms, and the importance to grain erosion of a natural mucoid coating, are noted

INTRODUCTION

This study was designed to examine the hydrography and the fluid-sediment interactions in an inlet floored with carbonate sand The approach adopted involved 1) describing the basic inlet geometry and the semi-permanent bedforms, 2) documenting the general flow field, 3) documenting the response of relatively small-scale bedforms to ebb and flood currents, and 4) conducting specific sand-tracer experiments

Morphologically speaking, the inlet studied is a specialized tidal channel that connects waters of the Florida Straits with a shallow lagoon about eight square miles in area (Fig 1) The lagoon is not enclosed, but opens to the Great Bahama Bank across a broad area of flats

---

[1]Contribution No 359 of the Virginia Institute of Marine Science

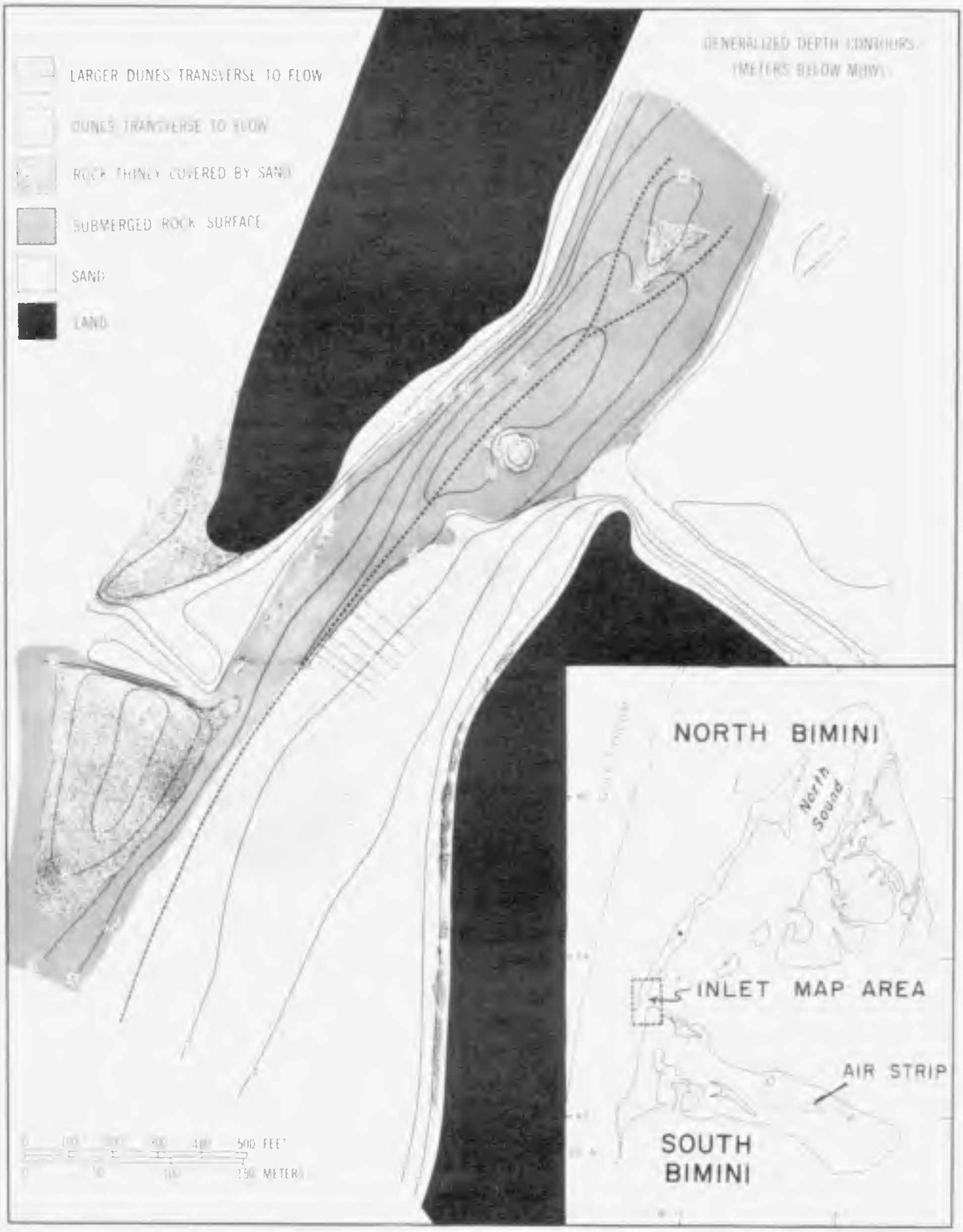

Figure 1.- Location, generalized bathymetry, and geology of Bimini Inlet channel.

Turekian (1957) felt that the lagoon was "host to three distinct water masses 1) an indigenous mass that moves in and out of the North Sound with the tides, 2) a mass entering from the Florida Straits through Entrance Point, and 3) a mass entering from the Bank" to the east

The tide range at Bimini varies between about 2 5 to 3 0 ft and sea level tends to rise or fall together at both Bimini and Miami (Wunsch, et al , 1969) Tides are of the semidiurnal type with a slight diurnal inequality Propagation of the tide wave through the open lagoon is such that the ebb flow (to the southwest) through the inlet is about 30 percent longer than the flood

Current speeds in the northern, constricted part of the inlet channel (Fig 1) are high enough to sweep sediment from the beachrock floor Some of the larger dunes in the central portion are composed of fragmented shell gravel This gives way to sand with median grain diameters of 0 6 to 0 8 mm in the southern portion of the channel Most of the grain surfaces in sand samples of shell hash taken from the central and southern portions of the inlet exhibit a glazed appearance when viewed under the binocular microscope Sand-grain surfaces become more chalky, however, as one moves lagoonward (Bathurst, 1967) The specific gravity of sand grains from eight samples in the area of "dunes transverse to flow" (Fig 1) was 2 84

During the period of study, November 5-13, 1967, water temperature in the inlet channel varied between 20° and 27°C, salinity between 34 and 38 ‰, and density between 1 0201 and 1 0267 g/cm^3 In May, 1955, Turekian (1957) found that salinity in the inlet varied between 36 0 and 37 0 ‰ and temperature ranged between 26 3 and 28 6°C over one tidal cycle

DETERMINATION OF INLET GEOMETRY

Existing nautical charts of the Bimini Islands (British Admiralty Surveys of the 1840's) inadequately define the inlet geometry Considering the general clarity of water at the inlet, it was decided to attempt bottom contouring by standard photogrammetric techniques

To provide horizontal control for aerotriangulation, a base line 2319 ft in length was established by electrotape Each end of the base line was pre-marked with a 4-x-4-ft , red plywood panel, the north end of the base being on North Bimini and the south end on South Bimini

Five vertical control points on land were also established and pre-marked in the same manner The levels were run with a Zeiss Opton level and were based on a tidal bench mark on North Bimini

The photography as planned placed some photo centers over water with land areas on only one side To facilitate the clearing of models during both aerotriangulation and compilation, seven floating targets (4-x-4-ft plywood) were anchored offshore to provide photographic images

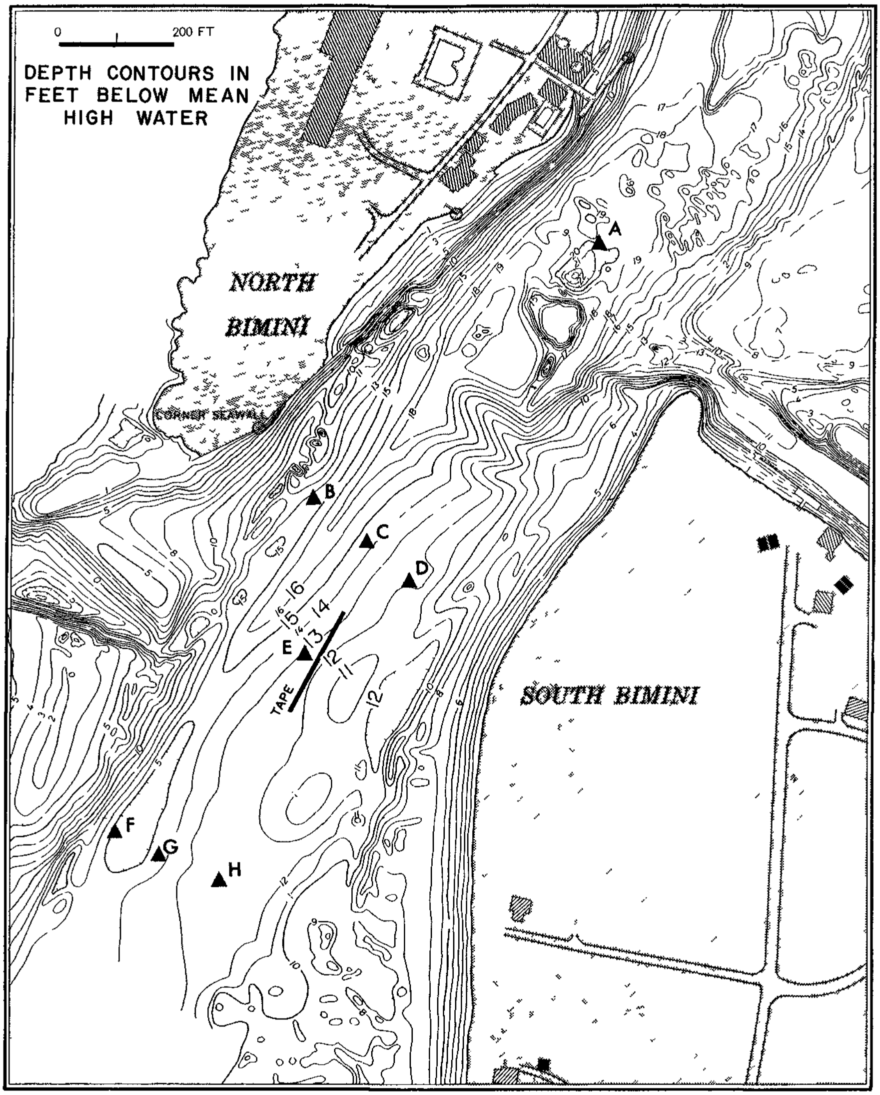

Figure 2 - Detailed bathymetry of inlet, locations of bottom-mounted sensor packages, and position of reference tape

A Wild RC-8 camera with a focal length of 152 29 mm, mounted in an Aerocommander aircraft, was used to obtain the photography on September 8, 1967 Film was Anscochrome D-200 with an ASA rating of 165 The flying height was 2000 ft above mean sea level, resulting in a photograph scale of approximately 1 4,000

Aerotriangulation was by stereoplanigraphic methods using drilled glass plates The contouring of the bottom (Fig 2) was accomplished on a Wild B-8 Plotter at 1 2,400 scale with a contour interval of one ft The average correction for the refraction index of water for the models contoured was 1 4

Hydrographic check lines run 45 days later indicated that the depth contours (Fig 2) were within ±0 25 to 0 5-ft for the shallow-water areas of the inlet The "larger dunes transverse to flow" (Fig 1) were adequately brought out in the bathymetric contours and the hydrographic check lines showed them to be essentially stationary over the 45 days that had elapsed since they were photographed

DOCUMENTATION OF FLUID PROPERTIES, WATER LEVEL, AND FLOW

Two tripod-mounted, "Geodyne" sensor packages were installed at each of the eight stations (A-H) shown on Figure 2 Each sensor package contained a platinum thermometer for measuring temperature, a torroidal cell for conductivity, a Savonius rotor for current speed, and a vane for current direction A given pair of instrument packages were mounted in the tripod so that the Savonius rotor of one was one ft above the bottom while that of its companion was eight ft above the bottom The mounting configuration was such that the flow pattern around a given rotor or vane was unaffected by the tripod legs or by the adjacent sensor package

Each tripod was placed on a level part of the bottom and the sensor packages were hardlined to one of four shore-based stations Each shore station contained a magnetic tape recorder and a radio transmitter A given sensor was interrogated every six minutes, each interrogation involving five separate readings of current direction and speed and one each of temperature, conductivity, and reference

Data from the four shore-based transmitters were sent by an RF link to a master station at the Lerner Marine Laboratory on North Bimini At the master station, all data from the 16 sensor packages were recorded sequentially on computer-compatible magnetic tape The entire system of sensors was continuously operated from 5 November through 13 November, 1967

A bubbler-type tide gage was installed on North Bimini, the orifice was attached to the tripod at Station B

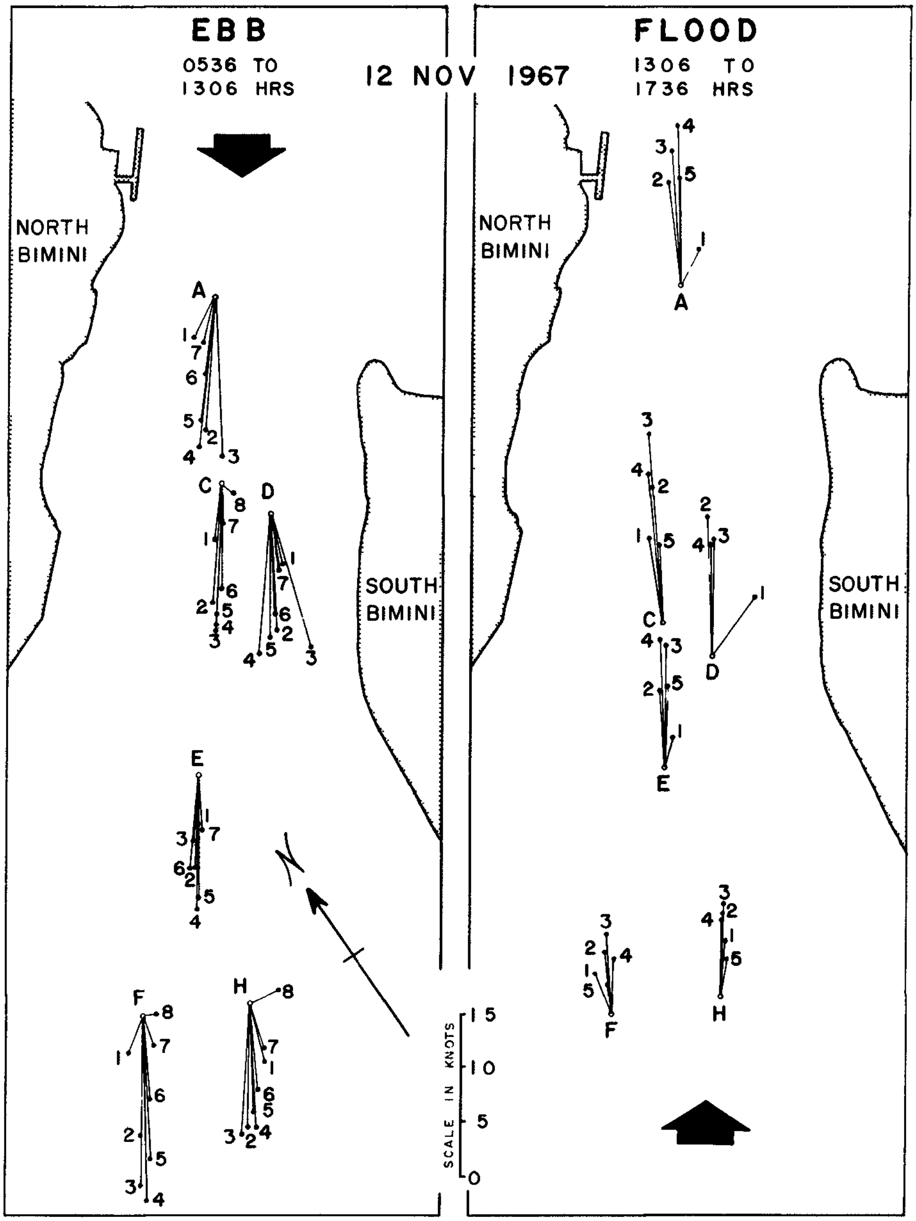

Figure 3 - Tidal-current vectors for a neap-tidal cycle (in hours after high-slack or low-slack water)

Data on maximum flow eight ft above the bottom are presented in Table 1 The absolute peak speed measured does not appear in Table 1 because it occurred prior to having all eight stations operational This peak speed was 4 1 knots and was measured eight ft above the bottom at Station A The time of measurement was during a maximum ebb flow that coincided with spring tides and a strong wind from the northeast that had been blowing for several hours

TABLE 1 - NEAR-SURFACE VELOCITIES AT SELECTED STATIONS (5 Nov 67, through 13 Nov 67) (F = flood current, toward NE into lagoon, E = ebb current)

SENSOR STATION (fig 2)	MAXIMUM VELOCITY (kts , flood or ebb) (direction, true)	TIME (date) (hours, EST)	AVERAGE MAXIMUM VELOCITY (kts)		AVERAGE DEPTH BELOW SURFACE TO ROTOR (ft) (All rotors eight ft above bottom)
			flood	ebb	
A	2 3 F 31°	5 XI 67 2142 hrs	1 7	1 7	10 5
C	2 8 E 190°	11 XI 67 0824 hrs	1 7	1 9	4 0
D	2 1 F 04°	6 XI 67 0936 hrs	1 3	1 5	2 7
E	2 2 E 213°	11 XI 67 0618 hrs	1 3	1 7	3 3
F	3 3 E 195°	11 XI 67 0824 hrs	1 0	2 0	5 7
H	2 6 E 234°	6 XI 67 0142 hrs	1 6	1 4	4 0

An idea of tidal-current speeds and directions during a neap-tide flood and ebb cycle may be obtained from the vectors of Figure 3 It is interesting to note that the directional spread is less than 21° (Station D, ebb) at all stations during relatively strong flows

An example of pulsations in the flow, for the upper rotor at Station E, is shown in Figure 4 Pulsations of this type were observed at all sensors and generally were of 12 or 18-minute frequency Spectral analysis with a boxcar window failed to reveal any obvious power at these relatively high frequencies Significant power was found at the tidal frequencies (6 7 and 12 3 hours) and at the sub-tidal frequency of 4 3 hours Power peaks of possible significance were also noted at all stations at frequencies of 2 4 and 3 2 hours

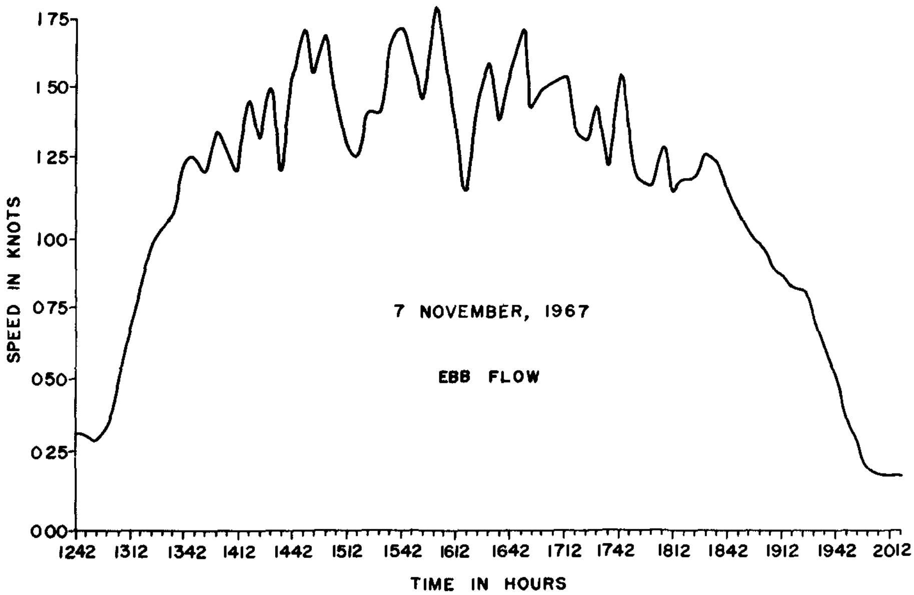

Figure 4 - Flow pulsations at upper rotor (eight feet off bottom) at Station E (Fig 2), during ebb flow

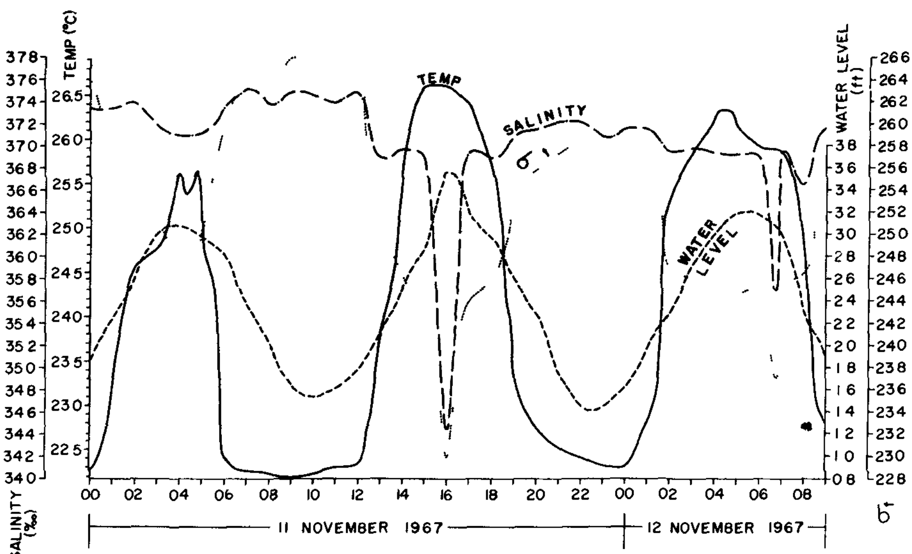

Figure 5 - Variation in salinity, temperature, and density (σt) at Station C (Fig 2), and water level at Station B, for 33 consecutive hours

A portion of the curves for variations in temperature, salinity, and sigma-tee at Station C and water level at Station B are plotted in Figure 5 The inverse relationship between sigma-tee and water level is due to the fact that in November, cooler, more-saline, high-density water flows out of the lagoon on ebb tide This water is completely replaced at high tide by warmer, lower-salinity, less-dense Gulf Stream water No density stratification was observed in this shallow channel of well-mixed waters

BEDFORM MORPHOLOGY

Measurement Procedures

The goal of the bedform monitoring program was to measure changes in geometry and position of the various forms through the reversing flow of one tidal cycle A fairly complete run was made on 13 November 1967 It started near the beginning of ebb flow and continued through one-half of the flood

Photographic techniques were the prime tools in making the bedform measurements Early in the survey a 200-ft , rigid tape measure (graduated in 1-ft intervals) was installed about one ft above the irregular bottom (Fig 2) About 15 ft to the west of the tape, and parallel to it, a wire guide-line was installed five ft above the bottom The guide-line served to maintain the diver-photographer at a uniform distance from the tape and allowed him to control his progress in the rather swift flow A second diver positioned himself behind the 200-ft tape The second diver pushed a fork-like device into the sediment so that the elevation of the bed relative to the tape measure could be photographed The fork device was composed of a series of 1/4-in rods welded at a 0 5-ft spacing to a rigid cross-member Each rod was graduated in 0 1-ft intervals The rigid cross-member had a bubble level cemented to it so that the upper member was horizontal, which in turn insured that the rods were vertical Two forks were used, each was six ft long and three ft high

A typical run was executed as follows Two divers would descend at the upstream end of the tape One diver would take the two forks to the tape and insert them, end to end, into the bed The photographer-diver then took a still picture from the guide-line position The other diver would then remove the upstream fork and place it in the downstream position for another photo, and so on A single-photograph sequence of the bedforms generally took thirty minutes Immediately before or after the still-camera sequence a run was made with a 16-mm movie camera From the developed still-camera sequence, the configuration of sand bed relative to horizontal was reconstructed

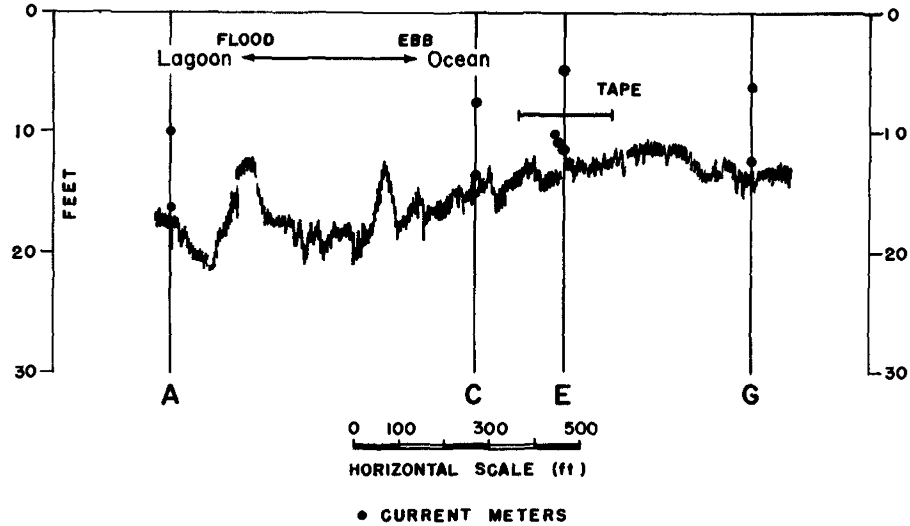

Figure 6 - Fathometer profile from sensor Stations A to C to E to G and vertical position of current meters

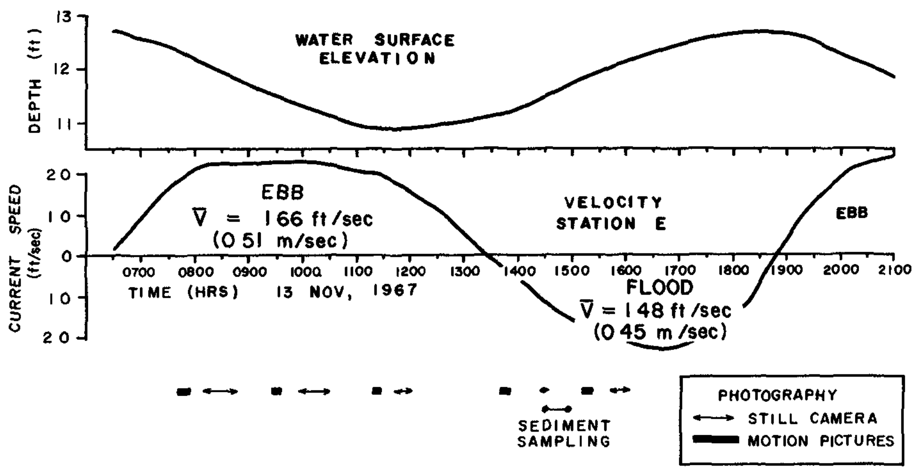

Figure 7 - Flow history and sampling times at Station E, 13 Nov , 1967

Field Setting

At any given time during the study three bedform length scales could be observed sand waves dunes, and ripples Inspection of Figure 1 shows that the sand waves exist only on the eastern side of the channel The dunes were long crested, the crest length being 10 to 15 times the wave length A fathometer run from stations A to C to E to G (Fig 2) is shown in Figure 6 There is a large rock outcrop at the northern end of the throat of the inlet, about 150 ft south of Station A A series of five sand waves had an average wave length of approximately 90 feet The fathometer profile shown was obtained during the slack water following a flood flow The fact that the ebb flow asymmetry still remains suggests that these bedforms are not strongly influenced by the flood flow Superimposed on these larger features were dunes and ripples that were modified by the reversing flow The position of the 200-ft tape is shown also, its northern end rests on the crest of the last sand wave Thus, the bedforms monitored included those in the lee of the sand wave crest, as well as those exposed to ebb flows of a converging nature Convergence was due to decreasing water depth in the direction of the southern end of the tape

The water surface time history and the velocity history at Station E on 13 November are shown in Figure 7 Also shown are the times when photographic sequences of the bedforms were obtained The velocity history illustrates the strong asymmetry in duration of the ebb relative to flood flow, which was found to be characteristic for this inlet The velocity history is at a mean relative depth ($z/\bar{d}$) of 0 66 (where z is the height of the rotor above the bottom and $\bar{d}$ is the mean water depth) The mean velocities (integrating over the flow duration) for the ebb and flood are, respectively, 1 66 ft/sec and 1 48 ft/sec In summary, we have a condition in which the ebb flow is generally stronger and of appreciably longer duration Net sediment transport may then be expected to be seaward

Evolution of Bedforms

The sequence of events in bedform change is shown schematically in Figure 8 where, for descriptive purposes, the cycle is started at the end of flood (Fig 8a) With the reversal of flow (Fig 8b), the bed sediment is transported up the steep gravity face of the dune to form what dimensionally might be considered the new dune crest A train of ripples also occurs on the dune flank These ripples are all of smaller amplitude than the one derived from the old edge of the dune crest The dominant ripple length is approximately 1 to 1 5 ft

With continued ebb flow the primary crest overtakes some of the other ripples in its lee There is a consequent increase in amplitude and the growing ripple slowly becomes a dune (Fig 8c) As the new dune crest advances (in the ebb flow direction, Fig 8d), the ripples in its lee become increasingly less active due to sheltering action Other ripples are then observed translating up the upcurrent flank of the dune These are of small amplitude and approximity 2 to 2 5-ft in length (Fig 8e, f)

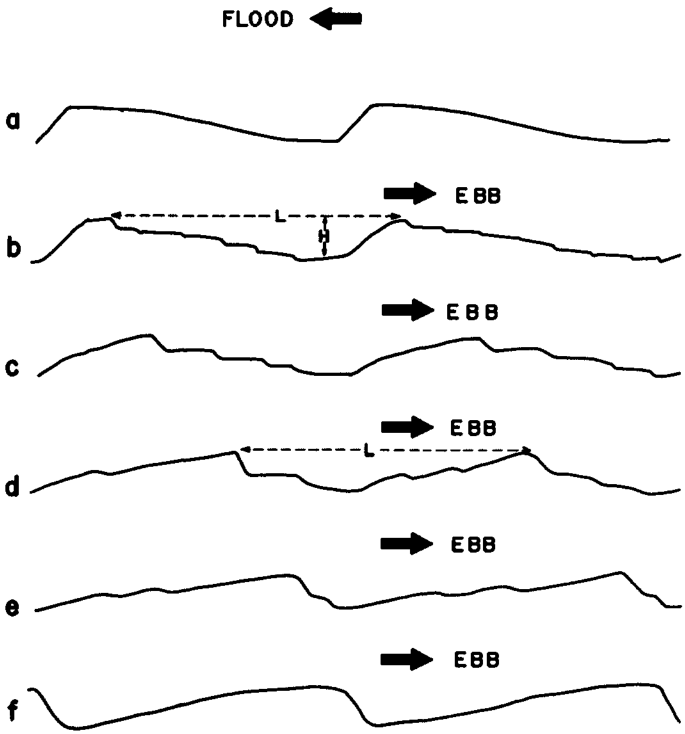

Figure 8 - Schematic bedform evolution

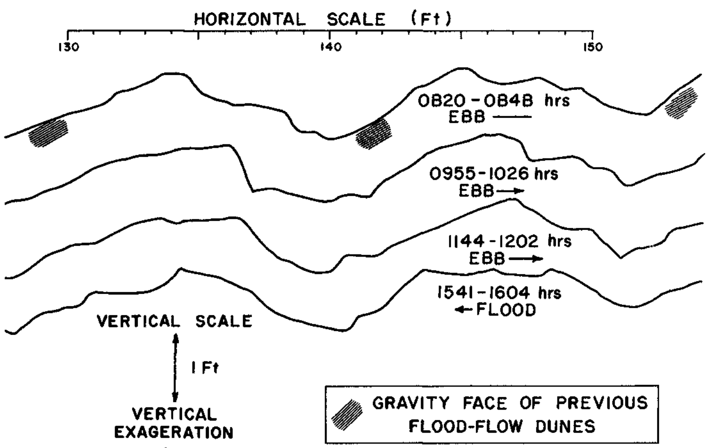

Figure 9 - Example of observed bedform changes during a tidal cycle

As the velocity of the ebb flow diminishes the dune crest slows its advance until bed transport stops, at which point the bedforms become dormant until the new flood flow is intense enough for grain transport Some of the measured bedform changes are shown in Figure 9 The flow conditions for the various sampling times may be noted in Figure 7

Throughout the study period visual observations indicated most of the sediment transport occurred via dune advance with no perceptible suspended load Given the aforementioned asymmetry in strength and duration of the flow (Fig 7) it might be expected that the ebb flow dune advance would be greater than the flood flow dune retreat This was observed to be the case over a three day period 10 November to 13 November Successive measurements of ebb-flow, dune-crest positions indicated a mean net advance out of the inlet on the order of 1 foot per tidal cycle This value is a very rough estimate as large variability was noted both in time and space

The evolving nature of the dunes presents some problems in determining length characteristics, however, as a flow cycle starts a reversal, a distinctive crest is generated on each dune This crest is the highest point above the downstream trough and it probably exerts a dominant influence on the gross wake characteristics for the dune The dune wave length (L) is defined as the distance between a given dominant crest and the next downstream crest Dune height (H) is defined as the vertical distance between the dominant crest elevation and the downstream trough

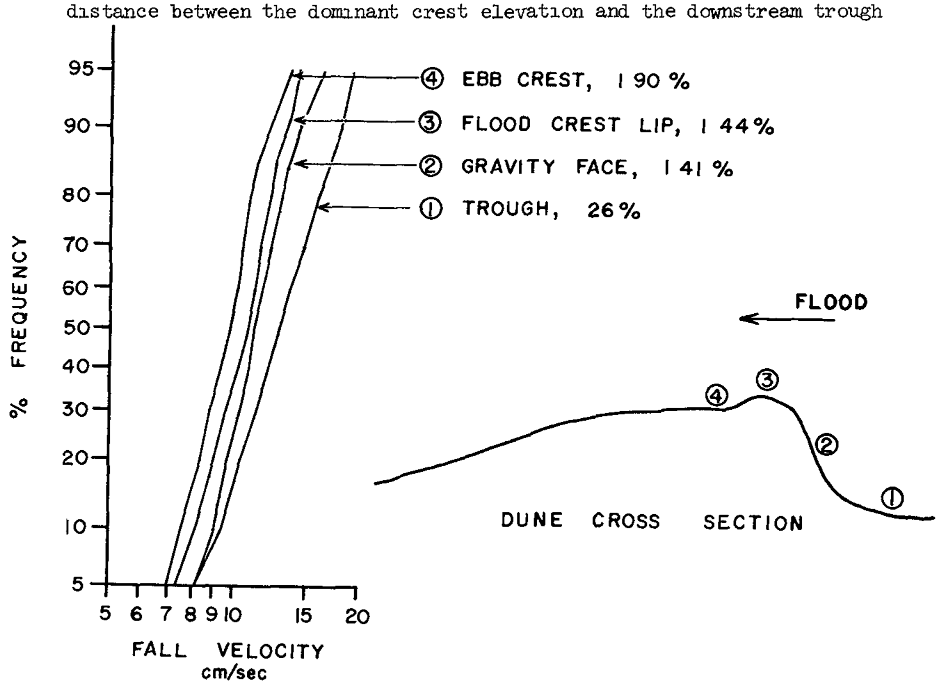

Figure 10 - Sediment fall velocity distributions Values represent % weight of material larger than 2 mm

Inspection of the bedform profiles over the 200-ft distance indicated that the wave lengths and heights were significantly different for the northern half (115 ft) of the tape as opposed to the southern half This is perhaps to be expected, as the first half encompasses those dunes which are formed in the lee of the large sand wave (see Fig 6) The results, cast as averages, are shown in Table 2 Two facts deserve specific comment First of all, it should be noted that during the ebb flow the dunes in the lee of the large sand wave have longer wave lengths and smaller heights than those beyond the direct influence of the sand wave There is only scanty evidence for the flood flow, but that available (1541-1604 hrs), suggests a uniformity in dune height The second point of interest is the relative stability of wave length and height (and, therefore, steepness) during the various phases of the reversing flow

TABLE 2 - SIZE PARAMETERS OF DUNES

Parameter	Position on Tape (Ft)	Time			
		0820-0848 hrs	0955-1022 hrs.	1144-1202 hrs	1541-1604 hr
$\bar{L}$ (ft)	0-110	14 3	14 0	14 3	15 6
Range of L		9 5-18 5	9 5-20 0	10 0-20 0	10 0-18 (
	110-200	10 7	10 9	11 3	10 5
		9 5-12 5	9 0-12 0	10 0-13 0	9 0-13 (
$\bar{H}$ (ft)	0-110	0 56	0 63	0 53	0 82
Range of H		0 27-1 10	0 25-1 4	0 25-1 20	0 25-1 [illegible]
	110-200	0 75	0 81	0 81	0 80
		0 50-1 00	0 60-1 00	0 5-1 00	0 50-1 (
$\overline{L/H}$	0-110	30	33	32	25
		8-41	9-68	11-50	12-64
	110-200	16	14	14	15
		12-26	11-20	10-23	11-25

Dune Field Sediments

Sediment samples were obtained on 13 November during flood flow, about one hour after flow reversal Samples were taken of the upper half-inch of the bed material on the dune flanks, crests, and troughs The trough samples are biased, as large fragments of the conch Strombis gigas were not collected Laboratory treatment consisted of a wet separation of the material greater than 2-mm, followed by a settling analysis of the finer fraction

All of the grain-size distributions from the settling analyses closely approximated a log-normal distribution with very little variation in the geometric standard deviation, $\sigma g = W_{84.1} - W_{50}$, which had an average value of about 1.2. The average median fall velocity of the trough material was about 12.6 cm/sec and at least 25 percent of the material (by weight) is larger than 2 mm. The sediments composing the dune flank and crest had a somewhat smaller median settling speed (10-11 cm/sec) and were generally less than 7 percent greater than 2 mm in mean size.

An example of these results is shown in Figure 10. The sequence shown was obtained during the flood flow when the flood crest was becoming established. Diver observations suggest that the small flood-flow crest is composed of material swept up the ebb-flow gravity face.

Flow Profile--Station E

In an attempt to obtain an estimate of the velocity profile over the dunes an auxiliary current-meter tripod containing two additional Savonius rotors was placed near Station E. Sampling of the rotors was synchronized with the two tripod-mounted Savonius-rotors and a sample of 46-seconds' duration was taken every six minutes. The relative positions of the four rotors are shown in Figure 6, the lowest rotor was about 1.5-ft. above the sand interface, the remaining rotors were 2.1, 3.2, and 8.3 ft. above the bottom.

During the ebb flow the rotor outputs indicated a larger speed near the bottom than that registered at the uppermost rotor (Fig. 6). This pattern persisted throughout the ebb flow until one-half hour before flow reversal at which time a normal profile was present. During the flood flow the enhancement of flow speed near the bottom was not present, instead, the flow was essentially uniform with depth.

It seems likely that the flow maximum near the bottom is a jet due to the sand wave field. The nature and development of jet flow over sand waves is being studied by J. Dungan Smith (Univ. of Washington). Smith (personal communication) has formulated a model predicting the jet and has documented jet occurrences in tidal flows. His early results indicate that the jet amplitude is a maximum when the sand wave height is about 20% of the water depth and that the jet is fully developed at the fifth wave in the field. The bedform conditions of the Bimini Inlet case described here are similar to those found by Smith. During flood flow the approach toward uniformity of velocity with depth is consistent with the fact the depth is then divergent downstream.

Discussion of Bedform Changes

Although past studies have delineated the significant variables that control bedform characteristics in unidirectional flow, there is no satisfactory formulation to predict the length and amplitude of bedforms found in the field. It may be anticipated that the problem is even more complex in the case of reversing tidal flow There are two main differences between the two cases In the case of tidal flows the time variations in stage (and discharge) for a given flow direction occur in a few hours and bedforms may not come into equilibrium with the maximum flow speeds Carey and Keller (1957), in a study of Mississippi River bedforms noted a bedform size dependence on discharge and postulate a lag between bedform change and change in stage Secondly, with the change in flow direction the flow may encounter (as in this study) an established bedform morphology of reverse symmetry The role of such initial conditions needs detailed attention

Aside from flow-acceleration effects, it may be anticipated that friction factors during a flow cycle will be somewhat different for reversing flows as opposed to a unidirectional flow of equivalent maximum velocity, because the character and position of the separation zone in the lee of the crest changes in time Model studies by Bayazit (1969) for ripples generated by reversing flows indicated friction factors less than those found for corresponding unidirectional flows The difference between the two cases was attributed to a possible lack of bedform equilibrium with the reversing flow In order to avoid the effects of acceleration, Bayazit used the maximum velocity in formulating a friction factor

In the absence of detailed studies it has frequently been assumed that bedform development in an inlet may not differ significantly from a corresponding steady flow (Bruun, 1966) If such was the case one might expect to find a progression from ripples to dunes as the velocity increases and the reverse order as the velocity decreases The present study indicates this view is probably oversimplified For this case, the basic bedform sizes are stable through time with the major changes being simply a reversal of dune geometry It is of interest to compare the dune lengths and heights observed here with those observed in unidirectional flow Analysis of field data by Allen (1968) showed that the characteristic lengths of dunes were strongly correlated with flow depth although it was recognized that dune size is not a unique function of depth Allen's relationships are, for lengths in meters

1) $H_D = 0\ 086 d^{1\ 19}$ and

2) $L_D = 1\ 16 d^{1\ 55}$

where H_D is dune height, d is flow depth and L_D is dune wave length Because there was relative stability in the average dune length and height during the observation period (Table 2), the mean depths over the two tape segments were used to calculate the expected values from equations 1 and 2 For the lagoon side of the tape the computed wave length is 35 6 ft whereas the observed mean value is approximately 14 5 ft The computed dune height is 1 6 ft and the observed mean is about 0 6 ft For the oceanside segment of the tape the computed wave length is 28 2 ft and the observed is about 11 0 ft, for dune heights we find 1 32 ft versus an observed value of about 0 80 ft The expected values from equations 1 and 2 are thus significantly larger than the observed mean values

Generally it can be said that the resulting scour is strongly influenced by the pile and the wave characteristics In most of the runs, very little to no bed movement could be observed away from the pile The pile served as a catalyst to start the scour activity and once started around the pile it spread over a large area and extended in some cases great distances from the pile Figs 9 and 10 show some typical scour patterns obtained from the experiments

CONCLUSIONS AND REMARKS

1 The critical velocity necessary to cause incipient motion in oscillatory flow appears to be lower than that for steady state flow

2 The ratio of the maximum velocity on the pile boundary and the initial free stream velocity, is less than the value of 2 0 for potential flow theory

3 Incipient motion on the pile boundary appears to be independent of $\frac{H}{h}$ and directly dependent on the parameters $\frac{h}{gT^2}$ and $\frac{d}{h}$

4 $\frac{\overline{Su}}{H}$ appears to be directly related to the sediment number N_s and the pile Reynold s Number N_{RP}

5 A maximum of only 6000 waves are required to reach an ultimate scour depth and in most cases 3000 waves are sufficient

6 The relative ultimate significant scour depth increases very rapidly at first, reaching three fourths of its ultimate depth in the first 1000 waves, and increases more slowly after that until it reaches its ultimate depth

7 Eddy forces, although initially influencing the scour patterns, do not appear to be of significance in the final scour pattern

8 The scour pattern resulting is primarily influenced by the pile and the wave characteristics

9 In all the scour experiments, the pile acted as a catalyst causing scour of the bed particles to be initiated whereas if the pile was not present little to no scour would have resulted

To try and predict scour depths for a prototype case or relate these unconclusive results to a prototype would be presumptuous To predict happenings or occurrences of a phenomenon in a prototype requires that there be similitude, both geometric and dynamic, between the model and prototype This requires that similitude exists between the orbital velocities and orbital lengths (i e wave characteristics are similar), grain size and grain size distribution in the bed, roughness of the beds, and translation of the orbit due to drift Without these similitudes erroneous conclusions could be reached in attempting to predict prototype conditions The difficulties in acquiring similitude between prototype and model were pointed out by Posey and Sybert[18] in their studies of scour around piles on offshore platforms It required several years of study and experimentation before actual prototype conditions were duplicated in the model

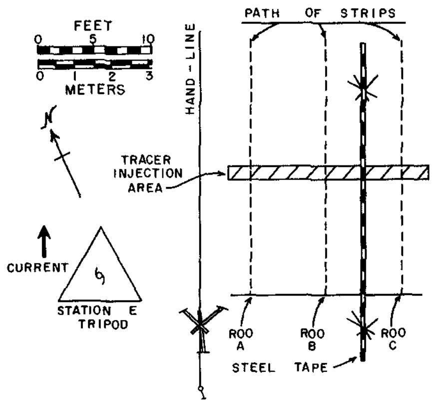

Figure 11 - Map View of Tracer Experiment Layout

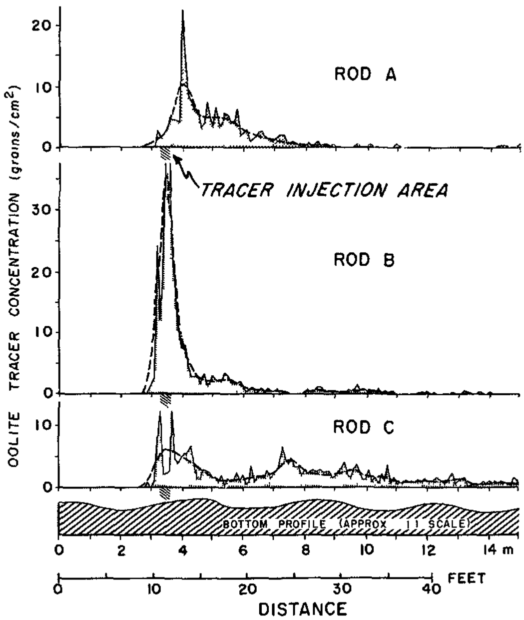

Figure 12 - Plot of Oolite Tracer Concentration versus Distance for Rods A, B, and C after the First Sampling Run

Plastic bags containing the tracers were placed within the injection area (Fig 11) by a diver who cut them open with a knife at the designated time of release Recovery of released tracers was accomplished using 0 15 x 18 m strips of K & E drafting film (Herculene) coated with Dow-Corning 103 compound These strips were unrolled on the bottom in a northerly direction parallel to a graduated steel tape Three strips, fixed at one end by steel rods were unrolled simultaneously by divers according to the configuration shown on Figure 11 Four sampling runs were made at 30-minute intervals beginning at 1307 hours

The recovered sampling strips were examined in the laboratory under ultraviolet light Tracers were counted within a 10 cm^2 grid placed over the strips at 0 1 m increments for the full length of the tape Tracer concentrations, expressed as the number of grains per cm^2, were then plotted against distance from the holding rods in meters Figure 12 is a plot of the initial sampling run for rods A, B, and C The dashed curves, intended for smoothing of the data, were obtained by dividing distance into 0 5 m class intervals and averaging grain concentrations therein

In examining the data, it was immediately apparent that the quartz grains (0 59-0 84 mm) were present in smaller amounts than the oolite (0 30-0 59 mm) and that their distribution was more limited A few quartz grains traveled as far as 15 m downstream in the first 30 minutes after the first release Most of the quartz tracers, however, assumed an almost normal distribution about a point less than 1 0 m downstream from the release zone The quartz tracers also appeared to be distributed uniformly in a lateral sense as evidenced by simultaneous comparisons between adjacent strips

Oolite tracers were recovered in greater numbers and their distribution appears to have been more widespread than that of the quartz material Following their release, significant concentrations of oolite ($\sim$ 1 grain/cm^2) were found at maximum distances from the release zone after 30 minutes, also the greater mass of these tracers, while remaining some 1-2 m downstream from the release zone, showed markedly skewed distributions toward the downstream side (Fig 12, Rods A and B) with pronounced bi- or trimodality in many cases (Fig 12, Rod C) Moreover, the oolite tracers often showed great lateral variability, as seen through the simultaneous comparisons of adjacent strips, and temporal variability, as seen in time-sequential comparisons along each of the strip paths

A bedform profile, obtained from photographs at the end of the flood current, is included in Figure 12 to show the relation of tracer concentration to bedforms

In order to quantify the observed lateral and temporal variability in oolite tracer distribution, a two-way analysis of variance (Rods versus Runs) was conducted using the oolite data of the four runs for rods A, B, and C The variable used in the analysis was tape distance in meters with

TABLE 3 - TWO-WAY ANALYSIS OF VARIANCE OF TRACER RECOVERY DATA (Variable is Tape Distance in Meters Tracer oolite)

ROD	SAMPLE	RUN 1	RUN 2	RUN 3	RUN 4
A	Mean	4 92	3 63	4 08	4 59
	Var	1 31	0 17	0 21	0 66
	Size	188	180	48	47
B	Mean	3 83	3 90	4 59	4 43
	Var	0 52	0 18	1 12	0 55
	Size	302	81	461	155
C	Mean	6 06	3 58	4 29	4 00
	Var	4 64	0 23	0 21	0 48
	Size	200	55	21	97

VARIATION SOURCE	SUMS of SQUARES	DEGREES of FREEDOM	MEAN SQUARE	F VALUE	CONFIDENCE LEVEL (PERCENTAGE)
TOTAL	2977 63	1834			
INTERACTION	459 05	6	76 51	67 41	> 99
ERROR	2074 00	1828	1 13		
ROD	178 52	2	89 26		
RUN	265 29	3	88 43		

the number of grains recovered at a particular distance serving as a frequency index for that distance Each sample of tape distances was therefore an indicator of the distribution of the tracer population for which a mean and a variance could be estimated

The object of the analysis was to determine whether or not tape distances could be pooled for all three rods and a separation of tape distance means effected between runs After the analysis was run, significant interaction indicated that pooling could not be done and therefore separation of the means was not possible Table 3 gives the results of this analysis

A similar analysis was attempted for the quartz tracers However, by using a one-way analysis of variance initially, it was learned that none of the means for runs could be separated due to their close similarity in value and the significant variance within each run This result only confirmed the visual impression that the quartz tracers evidenced very little bulk movement

DISCUSSION

The results obtained suggest that the oolite tracer exhibited a greater tendency toward transport than did the quartz tracer Probably the oolite tracer was "undersized" for the existing flow regime in the inlet while the quartz tracer was close to the prevailing grain sizes on dune crests Compared with the greater ebb current speed obtained at Station E (Av 1 7 knots, max 2 2 knots) it is not surprising that the flood current seemed to transport only a few quartz grains and that the distributions of these were less skewed Caution must be used in this interpretation, however, because the effect of burial of tracer grains is unknown due to the sampling method employed It has been instructive to the authors that an inlet such as the one at Bimini represents an extremely complex environment and even detailed measurements are inadequate for a clear picture of the way in which sand is transported For example, lateral variability of apparent grain motion was much more evident than anticipated, bottom transport is truly a three-dimensional problem

Although the results of the experiment are not conclusive, it seems evident that dunes play a major role in the distribution of tracer sands, and the modes of the concentration curves indicate points of grain accumulation which move slowly downcurrent with time In some cases, grains apparently travel very quickly over a succession of dunes, but a majority of samples indicate that most of them are fixed by the dune topography and therefore travel at much slower rates This slow transport is in keeping with the fact that the dunes themselves migrate very little during any given tidal cycle

The Bimini Inlet sediments appear to possess an organic coating (Bathurst, 1966) which did not allow most of them to adhere to the greased sampling strips All tracer grains were thoroughly dried and rewetted with detergent before release, they adhered very well to the strips Although mucoid coatings or gelatinous mats are not common to the active sands typical of the Bimini Inlet (Bathurst, 1966, p 90), there was clearly a difference in the surfaces of the _in-situ_ and tracer grains This then leaves the question of whether or not the _in-situ_ grains experience a binding effect that is not otherwise apparent

ACKNOWLEDGMENTS

All of the field work for this study was supported by the Atlantic Oceanographic and Meteorological Laboratories, of the Environmental Science Services Administration (ESSA), Miami, Florida Logistical support was obtained from the Lerner Marine Laboratory (American Museum of Natural History) on North Bimini Aerial photography and contour mapping was accomplished by the Photogrammetry Division, Coast and Geodetic Survey, ESSA

This study could not have been accomplished without the concerted efforts of many individuals We wish to express our great appreciation to Messrs F Beugnet, S Cofer, J Falkenhoff, B G Grant, C Kiersh, M P Lynch, E W Rayfield, G Reynolds, and D G Tyler for their efforts in the field R W Mathewson and his staff at the Lerner Laboratory were also most helpful in the field effort

REFERENCES

Allen, J R L 1968 The nature and origin of bedform hierarchies Sedimentology, 10 161-182

Bathurst, R G C 1967 Oolite films on low energy carbonate sand grains, Bimini lagoon, Bahamas Marine Geology, 5 89-109

Bayazit, M 1969 Resistance to reversing flows over movable beds Proc ASCE, Jour Hydraulics Div , 95(July 1109-1127)

Bruun, P 1966 Tidal Inlets and Littoral Drift, v 2, Skipnes Offsettrykkeri, Trondheim, Norway, p 1-193

Carey, W C and H D Keller 1957 Systematic changes in the beds of alluvial rivers Proc ASCE, Jour Hydraulic Div , 85(August 1-24)

Turekian, K K 1957 Salinity variations in sea water in the vicinity of Bimini, Bahamas, B W I , Amer Museum Novitates, No 1822, 12 pp

Wunsch, C , D V Hansen, and B D Zetler 1969 Fluctuations of the Florida current inferred from sea level records Deep Sea Research (Suppl) 16 447-470

Yasso, W E 1962 Fluorescent coatings on coarse sediments, an integrated system Office Naval Research, Geog Branch, Tech Rep 1, 48 pp